# An innovative wearable sensing system based on flexible piezoresistive sensors to estimate upper body joint angle using a Nonlinear AutoRegressive exogenous Neural Model

Abdo-Rahmane Anas Laaraibi, Corentin Depontailler, Gurvan Jodin, Damien Hoareau, Nicolas Bideau, Florence Razan

# An innovative wearable sensing system based on flexible piezoresistive sensors to estimate upper body joint angle using a Nonlinear AutoRegressive eXogenous Neural Model

Abdo-rahmane Anas Laaraibi, Corentin Depontailler, Gurvan Jodin, Damien Hoareau, Nicolas Bideau and Florence Razan

***Abstract*— The widespread adoption of instrumented textiles has made a significant impact in various domains, encompassing health monitoring, rehabilitation, biomechanics, and sports. This study specifically focuses on the development and evaluation of a smart garment that employs low-energy flexible sensors embedded within the fabric to effectively monitor upper body movements. These sensors utilize a piezoresistive polymer integrated into the garment and establish a connection with an electronic board for data acquisition. Wireless data transmission is achieved through the utilization of Bluetooth Low Energy (BLE) technology, with the garment showcasing an impressive average power consumption of approximately 10 $\mu$W. To ensure the sensor's performance and reliability, a comprehensive characterization process is meticulously conducted utilizing a dedicated test bench. Furthermore, this study conducts a comparative analysis between two distinct estimators utilized for determining the flexion/extension angles of the upper body joint. The first estimator leverages a Nonlinear AutoRegressive eXogenous (NARX) neural network model, while the second estimator employs a viscoelastic model. Through extensive evaluation, it becomes evident that the NARX neural network model outperforms the viscoelastic model, showcasing superior accuracy with a root-mean-square error of 4.85°. Consequently, the NARX neural network model emerges as the preferred option for accurately estimating the flexion/extension angles of the upper body joint.**

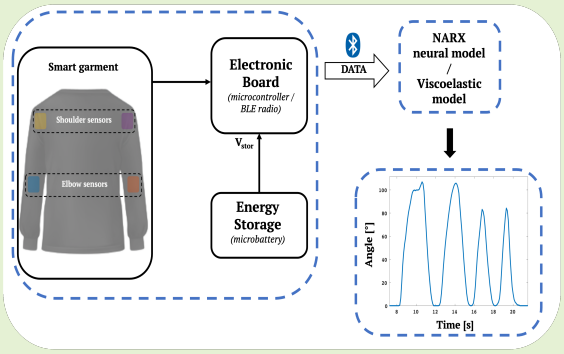


***Index Terms*— Wearable sensors, low-energy flexible sensors, smart garment, piezoresistive polymer, upper body movements, body joint angle, BLE, mechanical bending, IoT, NARX.**

## I. Introduction

THE popularity of wearable and flexible electronics is growing due to their ability to integrate with body movements, particularly in sports and health. Many applications utilize wearable technology to monitor sports activity [1], enhance quality of life, and prevent disease [2], [3]. These devices provide continuous monitoring of physical activities, health parameters and lifestyle, thanks to sensors to measure physiological parameters like heart rate, body temperature, and movements. However, the design and optimization of these systems present technical challenges that require innovative solutions and interdisciplinary collaboration.

Several alternatives to wearable technology for monitoring movements are available. These alternatives include video cameras, such as Kinect cameras [4], GPS and LPS technology like Catapult [5], optoelectronics systems like Vicon [6] and Qualisys [7], and motion sensors such as IMU sensors [8] and force/pressure sensors. Each alternative has its own advantages and limitations: video cameras (real-time, limited precision/range), GPS/LPS (accurate position, imprecise tracking), optoelectronics (high accuracy, complex setup), motion sensors (common, design challenges).

In addition to wearable technology, the integration of flexible sensors into garments for monitoring human motion offers significant advantages. Various types of flexible sensors, including capacitive sensors [9], fiber optic polymers [10], piezoelectric sensors [11], and piezoresistive polymers [12], have undergone

This study was funded by the ANR within the framework of the PIA EUR DIGISPORT project (ANR-18-EURE-0022)

Abdo-Rahmane Anas Laaraibi and Florence Razan are with OASIS, IETR UMR CNRS 6164, Université de Rennes 1, 35042 Rennes, France, and also with the Department of Mechatronics, and the SATIE Laboratory, UMR CNRS 8029, École Normale Supérieure de Rennes, 35170 Bruz, France (e-mail: abdo-rahmane-anas.laaraibi@ ens-rennes.fr; florence.razan@ens-rennes.fr).

Corentin Depontailler is with the Department of Mechatronics, École Normale Supérieure de Rennes, 35170 Bruz, France (e-mail: corentin.depontailler@ens-rennes.fr).

Gurvan Jodin and Damien Hoareau are with the Department of Mechatronics and the SATIE Laboratory, UMR CNRS 8029, École Normale Supérieure de Rennes, 35170 Bruz, France (e-mail: gurvan.jodin@ens-rennes.fr; damien.hoareau@ens-rennes.fr).

Nicolas Bideau is with the Movement, Sports and Health (M2S) Laboratory, École Normale Supérieure de Rennes, 35170 Bruz, France (e-mail: nicolas.bideau@univ-rennes2.fr).

extensive research and have been proven effective in accurately sensing pressure or strain to monitor movement.

Yu et al. [13] discussed the development of a novel type of flexible, wearable capacitive pressure sensor aimed at recognizing human motion states. The article recognizes that the effectiveness of flexible sensors in recognition has been limited by factors such as sensor sensitivity and stability. Accurately discerning changes in capacitance values of the sensor has also been a challenging task due to noise interference. Wang et al. [14] presented the development of a stretchable optical fiber sensor made with graphene and PDMS. The sensor is capable of detecting human movement and has potential applications in health monitoring systems. However, the article mentions that the sensor's sensitivity may be affected by temperature changes, and its performance may degrade over time due to environmental factors. Mokhtari et al. [15] discussed the potential of nanostructured piezoelectric fibers in smart garments, focusing on applications such as energy harvesting and force measurement. The article acknowledges the challenges associated with widespread adoption and emphasizes the need to enhance durability, washability, and comfort for long-term viability. Zhang et al. [16] proposed a method for capturing and recognizing human arm/hand gestures using flexible strain sensors. However, the study acknowledges several challenges in the field, including the need to address inconsistencies in capturing dynamic behaviors and the lack of accurate gesture recognition techniques. Abro et al. [17] conducted a study on a flexible smart garment integrating flex sensors to monitor body postures. The study emphasizes the benefits of flex sensors but also reveals important limitations in the smart garment context. Notably, flex sensors cannot withstand washing, have a restricted range of motion, and are unidirectional. Furthermore, their fragility poses an additional drawback.

Recent research has demonstrated exceptional detection performance; however, the seamless integration of the technology has not yet been fully optimized, and certain commercial solutions have been constrained by price or performance limitations. Notwithstanding these constraints, piezoresistive sensors have garnered significant popularity in various scientific advancements due to their cost-effectiveness and flexibility. Consequently, they are well-suited to fulfill the current requirements for human motion detection.

Our manuscript focuses on the development of a low-cost and portable sensing system utilizing flexible piezoresistive sensors to estimate the angle of the upper body joint. Our approach entails comparing different models to comprehensively analyze the data acquired by the sensors, enabling us to deliver precise and reliable angle measurements.

The article begins by introducing a garment incorporating piezoresistive sensors connected to an electronic board, ensuring the system's portability. We demonstrate the garment's capability to detect resistance changes corresponding to alterations in joint angles while simultaneously examining the system's energy consumption. Subsequently, we describe the design and characterization process of the piezoresistive sensors, which comprise a piezoresistive elastomer and a conductive textile. These sensors are integrated into a fabric and sewn using a sewing machine, after which they undergo comprehensive characterization on a dedicated test bench. The resulting solution is not only cost-effective but also reliable, enabling resistance measurements of the sensors during static and dynamic movements. The paper concludes with a comparative analysis of two models: a neural network model and a viscoelastic model. We assess their effectiveness in estimating the bending angle of the upper body based on the measured resistance.

## II. System Description

### A. Description of the piezoresistive effect

The piezoresistive effect is a change in the electrical resistivity of a material when mechanical stress is applied, as illustrated in Fig. 1. In other words, the application of mechanical pressure, tension, or bending decreases the distance between charge particles within the Velostat and increases the number of conductive paths, leading to resistance variations.

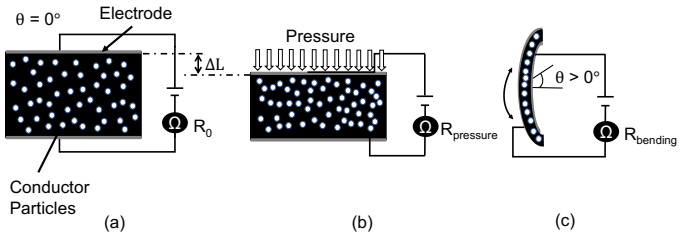


Fig. 1: Velostat diagram with particles inside the material are represented by white circles, **(a)** normal state; (**b**) with pressure; and **(c)** mechanical bending.

The designed sensor is based on a single layer of polyolefins carbon black, namely, Velostat (3M Electronics division, Saint Paul, USA) [18]. It is a piezoresistive material made of polymer sheet and having a high resistivity (<500 Ωcm). It can be used in flexible electronics, portable electronics and matrix sensors.

The sensitivity of the Velostat to applied pressure is mainly defined by two physical factors: quantum tunneling and percolation [19].

Quantum tunneling affects the conductivity of a composite material when the distance between the conductive particles inside the polymeric materials varies due to the applied pressure, which deforms the material. Therefore, the particles in the Velostat interact electrically through interparticle tunneling.

The percolation is related to a change in conductivity between the insulating and the conductive state of a material caused by the change of applied pressure.

The system's complete resistance consists of two parts: a) the contact resistance between the electrodes and the piezoresistive polymer, and b) the piezoresistive effect. This results in a significant change in resistance when we manipulate the sensor, providing it with the sensitivity to detect the application of a load (i.e., applied pressure or mechanical deformation).

### B. Smart Garment

*1) Sensors description:* Our proposed smart garment comprises four embedded piezoresistive sensors. Each sensor design adopts a sandwich structure consisting of five layers, as illustrated in Fig. 2.

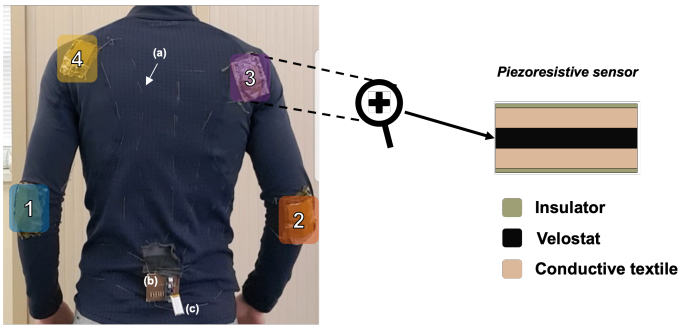


Fig. 2: An in-depth look at the smart garment using piezoresistive sensors: (1), (2): Sensors on elbows; (3), (4): Sensors on shoulders; **(a)**: Conductor wires; **(b)**: Electronic board; **(c)**: Battery.

The sensor construction begins with a layer of Velostat positioned at the middle, with two conductive textile tapes placed above and below the Velostat.

The conductive textile material used is obtained from an A4 sheet of silver-plated knitted fabric (STATEX Shieldex® Technik-tex P130 + B [20]). It is composed of 78% Polyamide and 22% Elastomer, serving as electrodes to provide the necessary voltage to the piezoresistive material.

To ensure optimal contact between the electrodes and Velostat, a non-conductive thread has been used to sew the conductive textile onto the piezoresistive material. Furthermore, we have incorporated a layer of polyimide, specifically Kapton®, which serves two crucial purposes:

- Firstly, the inclusion of Kapton minimizes potential interference in voltage changes, ensuring precise and accurate sensor readings. By reducing external disturbances, we can obtain reliable data on the garment's movement detection capabilities;
- Secondly, Kapton acts as a protective barrier, effectively isolating the sensors from the external environment. This shielding helps safeguard the sensors from potential damage or contamination, thereby prolonging their lifespan and maintaining their functionality over time.

These sensors demonstrate dynamic resistance changes across a defined mechanical angular range spanning from 5 to 160 degrees. Furthermore, in accordance with prior research [21], it has been established that these sensors also exhibit sensitivity to pressure.

*2) Sensors positioning on the garment:* Proper placement of the sensors on the garment is crucial for identifying areas where mechanical bending can be applied to the sensors. For this study, we opted to integrate the sensors at the back of the shoulders and on the elbows. Fig. 2 illustrates the sensor locations on the garment.

The dimensions of the sensors have been chosen in relation to the studied zone in order to capture the pressure and the mechanical flexion of the elbows and the shoulders. For this reason, the elbow sensors are 10 cm x 7 cm and the shoulder sensors are 7 cm x 5 cm. The designed piezoresistive sensors are sewn with classic sewing thread on the garment. Moreover, the electrical connection of the sensors with the electronic board is made by winding the conductive wires around the copper areas on both the top and bottom layers.

The smart garment composed of 4 piezoresistive sensors ($N_s = 4$) validates the presence of motion by simply detecting changes in resistance. To capture the signals, a customized printed circuit board (PCB) has been developed. It incorporates a voltage divider bridge to convert the resistance variation (output from the piezoresistive sensors) into voltage changes. Additionally, an electronic board, namely the Nano 33 BLE (Arduino, Ivrea, Italy), equipped with an analog-to-digital converter (ADC) and a Bluetooth module is integrated to transmit the converted data to a laptop running a custom algorithm within the MATLAB environment.

*3) Dynamic behavior and quantitative results:* In the analysis of the garment-based detection system depicted in Fig. 3, changes in normalized resistance values ($N_r$) serve as crucial indicators of movement. The normalized resistance is a criterion defined as follows $N_r^i = \max(R_{sensor}^i, 300\Omega)/300\Omega$, with $R_{sensor}^i$ the i-th sensor resistance. These values are reliable indicators used to trigger detection when $N_r$ falls below 1, indicating significant motion in the corresponding joint. To ensure the accuracy of the motion data, a sampling frequency of 10 Hz was employed to capture the sensor signals. The dataset used for analysis comprises 700 data samples. However, to maintain space and improve clarity, only 265 representative samples are presented in the Fig. 3.

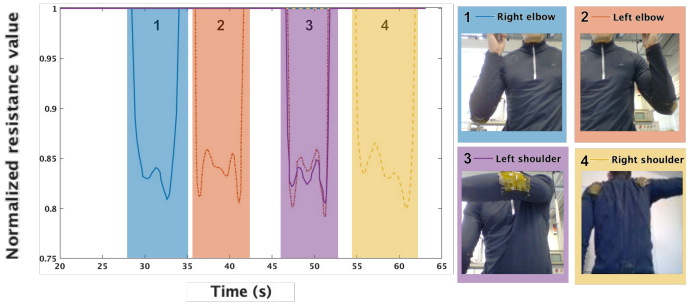


Fig. 3: Motion Detection via Embedded Sensors in Garment: (1) Right Elbow, (2) Left Elbow, (3) Left Shoulder, and (4) Right Shoulder, leveraging changes in normalized resistance values ($N_r$) as indicators of movement; triggering detection when $N_r$ is less than 1.

Fig. 3 (1) illustrates the observed detection in the right elbow sensor (blue area) during a 135° flexion. Similarly, the red area in Fig. 3 (2) depicts the response of the left elbow sensor to the same flexion. It is important to note that a value of $N_r$ less than 1 indicates the detection of a flexion.

Fig. 3 (3) illustrates the movement of the left shoulder and a 90° flexion of the left elbow, resulting in a decrease in resistance in both the shoulder and elbow sensors. This change is visually represented by the purple area.

On the other hand, Fig. 3 (4) displays the movement of the right shoulder (yellow area), which differs from that of the left shoulder. In this scenario, the right elbow remains unflexed, maintaining its initial position at 0°. Consequently, the variation in resistance is only detected by the right shoulder sensor.

The normalized resistance evolution from Fig. 3 demonstrates

the potential of integrating flexible sensors into clothing to detect movement, specifically changes in angle. The remainder of the article focuses on a methodology to reconstruct the rotational angle from resistance measurements obtained from a single sensor.

*4) Resistance measurement technique:* As presented on the electrical diagram on Fig. 4, resistance measurements are made through the General Purpose Input/Output (GPIO) ports using a voltage divider bridge, placing the sensor resistance, $R^i_{sensor}$, in series with a fixed known reference resistor, $R_{ref}$. The analog input voltage of the analog to digital converter ($V^i_{out}$) is linked to the resistance by equation (1).

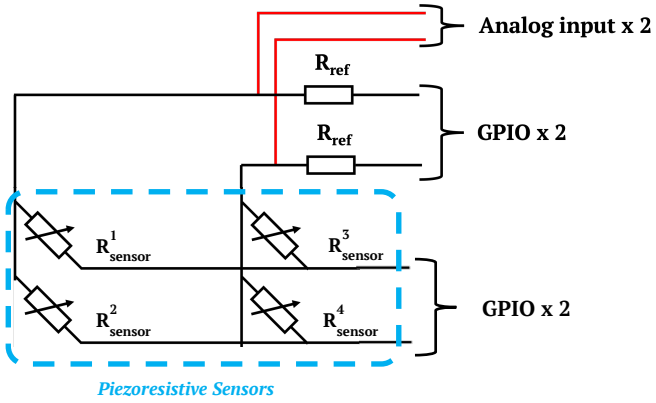


Fig. 4: Measuring Resistance with GPIO: Voltage Divider Bridge Method in Action

$$V^i_{out} = V_{in} \cdot \frac{R^i_{sensor}}{R^i_{sensor} + R_{ref}}, \tag{1}$$

Where, $V^i_{out}$ the voltage at the sensor, $V_{in}$ the supply voltage, $R^i_{sensor}$ the i-th sensor resistance and $R_{ref}$ the reference resistor.

A 470Ω reference resistor $R_{ref}$ is chosen to maximize the output voltage amplitude across the entire $R^i_{sensor}$ range of 10KΩ to 100Ω.

### C. System energy consumption

The analysis of the system's energy consumption involves estimating the average power consumption for each transmitted data frame between the system and the laptop and calculating the operating time. The average power of the system, denoted as $P_{av}$, is determined using Equation (2) and is found to be 56 mW.

$$P_{av} = \frac{1}{\tau} \int_0^{\tau} V_{stor}(t) \cdot I_{syst}(t) \cdot \mathrm{d}t, \tag{2}$$

The time interval between 0 and $\tau$ which is used to calculate the average power, corresponds to a whole number of program operation periods once the system reaches a steady state.

As explained in Section II-B.4, the sensors are powered by GPIOs through a bridge divider. The GPIOs alternate driving the voltage dividers to interrogate all the sensors, with an interrogation duration of $t_{on}$ = 750 $\mu$s occurring every 100 ms. To save energy, the GPIOs are not driven most of the time.

The average power consumption of the garment sensors, denoted as $P_{av,garment}$, is indeed 10 $\mu$W, as given by Equation (3).

$$P_{av,garment}(t) = \frac{1}{\tau} \sum_{i=1}^{N_s} \frac{V^2_{in}(t)}{R_{ref} + R^i_{sensor}(t)} \cdot \frac{t_{on}}{N_s}, \tag{3}$$

In this equation, $N_s$ is the total number of sensors, and $R^i_{sensor}$ represents the resistance of the i-th sensor.

Furthermore, the developed smart garment is equipped with a rechargeable lithium-ion battery consisting of a single cell with nominal characteristics of 3.7V and 380mAh. With the observed power consumption, the battery can ensure a lifetime of 25 hours, which corresponds to over 3 days of daily use for 8 hours each day.

## III. Characterization of Piezoresistive Sensors and Experimental Setup

### A. Design of piezoresistive sensors

In this section, we provide a comprehensive characterization of a piezoresistive textile sensor, aiming to gain a deeper understanding of the material's behavior and establish a link between the sensor's resistance measurements and the bending angle. The tested sensor design follows a sandwich structure, as depicted in Fig. 5.


Fig. 5: Manufacturing of a piezoresistive sensor with electrodes made of conductive textile material: **(a)** The 5 layers of the sensor, where (1) is the conductive textile tape (0.55 mm), (2) the polyamide elastane fabric, (3) the conductor wire and (4) the piezoresistive layer (0.1 mm thick); **(b)** The sandwich structure before final closing.

### B. Experimental setup

*1) Electromechanical characterization of conductive textile alone:* Prior to characterizing the realized piezoresistive sensor, we conduct thorough static and dynamic studies on the conductive textile alone.

These studies serve as a crucial foundation for understanding the behavior and properties of the conductive textile, which

plays an integral role in the sensor. By examining the conductive textile in isolation, we gain valuable insights into its electrical conductivity, mechanical stability, and performance under various conditions. This preliminary analysis ensures a comprehensive understanding of the conductive textile's characteristics, forming a solid basis for subsequent characterization and evaluation of the complete piezoresistive sensor.

The static characterization involves subjecting the conductive textile strip to a tensile test on a specialized test bench, as depicted in Fig. 6. This test allows us to study the behavior of the textile and record its resistance as a function of the length of stretching. To measure the variation in resistance, we utilize the analog output of an Arduino through a voltage divider bridge, as explained in section III-B.2. Simultaneously, the length of stretching is determined using an ultrasonic telemeter, ensuring accurate data collection.

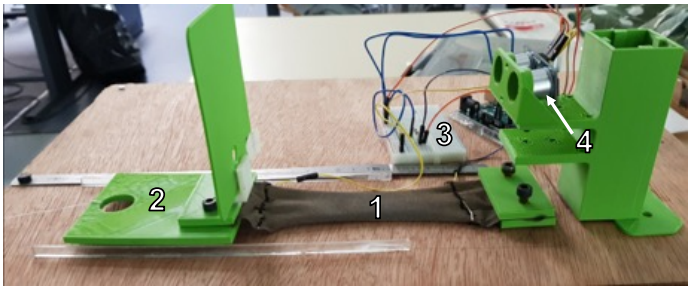


Fig. 6: Test bench made to measure resistance and strain: **(1)** Conductive textile (10 cm x 5 cm), **(2)** Sliding guide, **(3)** Acquisition board, **(4)** Ultrasonic sensor.

In the dynamic study, we sew the conductive textile onto the garment at the elbows, enabling us to capture real-time data. The recorded information is then transmitted wirelessly via Bluetooth Low Energy (BLE), facilitating convenient and seamless communication between the sensor and other devices or applications. This dynamic study provides insights into the behavior of the conductive textile during movement and allows for the evaluation of its performance in practical scenarios.

*2) Electromechanical characterization of piezoresistive sensors:* Following the characterization of the conductive textile and gaining an understanding of its behavior, we proceed to characterize the developed piezoresistive sensor in the section III-A on a dedicated test bench. During this characterization, we record both the resistance and bending angle of the sensor using a specially designed plastic instrumented hinge. This hinge is constructed using 3D printed PLA and laser cut acrylic, ensuring its precision and durability.

To measure the bending angle, a potentiometer is securely attached at the center of the joint. Its initial position corresponds to a bending angle of 0°, providing a reference point for further measurements. As the sensor undergoes bending or flexing, the potentiometer captures the changes in the bending angle, allowing us to accurately quantify and record the sensor's response.

The experimental device depicted in Fig. 7 consists of several components that play specific roles in the characterization process. It includes a rotating joint (2) responsible for applying

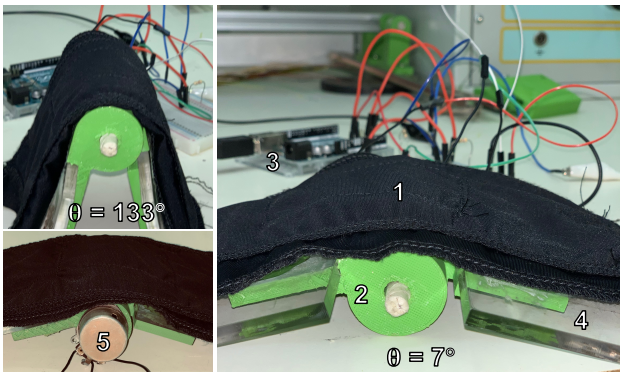


Fig. 7: The joint for the characterization of the piezoresistive sensor as a function of the angle, **(1)** the piezoresistive sensor, **(2)** 3D printed hinge, **(3)** Acquisition board, **(4)** acrylic, **(5)** potentiometer.

mechanical bending to the tested piezoresistive sensor (1). Additionally, a reference angle sensor in the form of a potentiometer (5) is incorporated to measure the angle of rotation, denoted as $\theta$. The acquisition card (3) is utilized to collect and process data from the sensor.

During the process of characterization, the electrical resistance of the piezoresistive sensor is precisely measured utilizing an Arduino board, specifically designated as $R_{bending}$. This measurement procedure offers valuable insights into the sensor's electrical characteristics and its behavior when subjected to mechanical bending. To accurately determine the resistance of the sensor, a voltage divider configuration was employed, as visually depicted in Fig. 8. The corresponding mathematical equation utilized for this determination is represented as Equation 4.

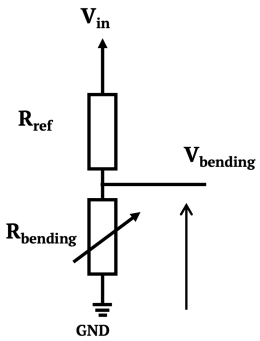


Fig. 8: Illustration of a Voltage Divider Circuit with a Fixed Reference Resistor ($R_{ref} = 470\Omega$) and Sensor Resistance ($R_{bending}$), demonstrating the Supply Voltage ($V_{in}$) and Voltage at the Sensor ($V_{bending}$).

$$R_{bending} = R_{ref} \cdot \frac{V_{bending}}{V_{in} + V_{bending}}, \tag{4}$$

## IV. Modeling of Piezoresistive Sensors

This section utilizes two distinct methods to determine the mechanical bending based on the electrical resistance of the sensors. The first approach employs viscoelastic modeling,

while the second approach utilizes a neural network model known as Nonlinear AutoRegressive eXogenous (NARX). Both models have been developed utilizing a single dataset containing 6057 samples, all collected at a consistent sampling rate of 10 Hz.

The source code and datasets are available on the following open-source repository: `https://gitlab.com/satie.sete/flexangleestimate`.

Further comparison between predicted data and measured data for both models has been performed in this paper using the Root Mean Square Error (RMSE) and the normalized error through equations (5) and (6) respectively.

$$RMSE = \sqrt{MSE} = \sqrt{\frac{\sum_1^\tau (\theta^i - \hat{\theta}^i)^2}{\tau}} \tag{5}$$

$$err(\%) = \frac{\theta - \hat{\theta}}{160} \cdot 100 \tag{6}$$

Where $\theta$ is the measured reference angle by the test bench, and $\hat{\theta}$ is the angle estimated by both models. The normalization is relative to the maximum observed rotation, i.e., 160°.

The overall view of the modeling of piezoresistive sensors section is represented by the diagram in Fig. 9.

### A. Viscoelastic model

Due to the nature of the polymer, which is a viscoelastic material, the resistance of this sensor is a function of the material properties of the polymer composite, the mechanical bending and the strain. The modeling is decomposed twofold, as illustrated in Fig. 10. Linear dynamic viscoelasticity and time-independent nonlinear piezoresistive relationship are assumed.

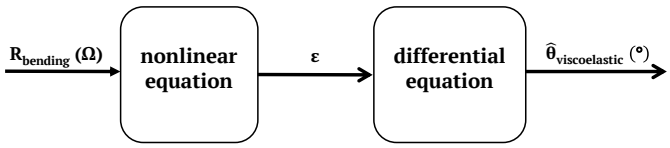


Fig. 10: The viscoelastic model of electrical resistance as a function of strain $\varepsilon$ and bending angle $\hat{\theta}_{viscoelastic}$.

In our case, a phenomenological approach is used to describe the relationship between an imposed bending angle, denoted as $\hat{\theta}_{viscoelastic}$, and the corresponding damped response of the resistance as a function of the strain, denoted as $\varepsilon$. As shown in Fig. 11, this relationship is characterized by a nonlinear function proposed in equation (7). Additionally, a set of differential equations, proposed in equations (8), (9), and (10), relate the bending angle to the strain.

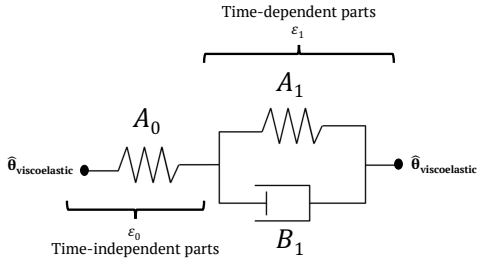


Fig. 11: Standard Linear Solid (SLS) model.

$$R_{bending} = R_0 \cdot (1 - \varepsilon) \cdot e^{-\gamma \cdot \varepsilon}, \tag{7}$$

where, $R_{bending}$ denotes the resistance of the sensor, $R_0$ the initial resistance, $\varepsilon$ the strain, and $\gamma$ the relaxation parameter.

$$\varepsilon = \varepsilon_0 + \varepsilon_1, \tag{8}$$

$$\hat{\theta}_{viscoelastic} = (A_1 \cdot \varepsilon_1) + (B_1 \cdot \dot{\varepsilon_1}), \tag{9}$$

$$\hat{\theta}_{viscoelastic} = A_0 \cdot \varepsilon_0, \tag{10}$$

where, $\hat{\theta}_{viscoelastic}$ the bending angle, $A_0$, $A_1$ and $B_1$ the internal variables of the viscoelastic model.

In this study, we have employed the viscoelastic model described by [21] to estimate the bending angle applied to the sensors.

To estimate the model's bending angle $\hat{\theta}_{viscoelastic}$ shown in Fig. 10, we require the parameter values $A_0, A_1, B_1$, and $\gamma$ illustrated in Fig. 11. To determine these values, we formulated an optimization problem as presented in Equation 11. To solve this problem, we utilized MathWorks MATLAB with the Genetic Algorithm solver.

The four parameters ($A_0, A_1, B_1$, and $\gamma$) were optimized by minimizing the mean square error (MSE) using Equation 11 between the measured bending angle $\theta$ on the test bench and the bending angle $\hat{\theta}_{viscoelastic}$ calculated by our algorithm 1.

$$\underset{x}{\text{minimize}} \quad f_0(x) = \sum_{i=0}^{\tau} ||\theta^i - \hat{\theta}^i_{viscoelastic}(x)||^2 \tag{11}$$

Starting with Algorithm 1, we first determined the strain $\varepsilon$ as a function of $R_{bending}$, $R_0$, and $\gamma$ using Equation 7 through the trust region dogleg method available in MathWorks MATLAB 2023a software.

Subsequently, we applied the implicit Euler method to solve the standard linear solid model described by Equations 9 and 10 in order to find the bending angle $\hat{\theta}_{viscoelastic}$.

### B. NARX Model

The NARX (Nonlinear AutoRegressive eXogenous) concept is an extension of the Autoregressive Exogenous (ARX) approach, which is a commonly used technique for identifying linear black box systems. NARX models are a type of recurrent dynamic neural network that are well-suited for modeling a

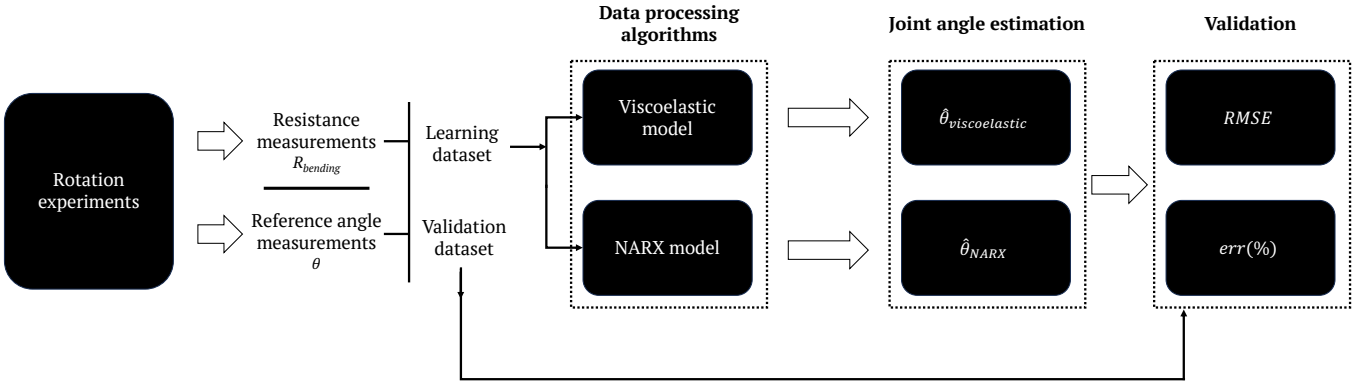


Fig. 9: Comprehensive diagram for modeling piezoresistive sensors.

**Algorithm 1** Viscoelastic model

find $\varepsilon$ in function of $R_{bending}$, $R_0$ and $\gamma$
**for** $i = 1, 2, \ldots, size(t)$ **do**
  $\varepsilon(i+1) = \varepsilon(i)$
  $A_0(i) = (A_{0a} \cdot \hat{\theta}_{viscoelastic}(i)) + A_{0b}$
    ▷ Elastic modulus of the spring $A_0$
  $A_1(i) = (A_{1a} \cdot \hat{\theta}_{viscoelastic}(i)) + A_{1b}$
    ▷ Elastic modulus of the spring $A_1$
  $B_1(i) = (B_{1a} \cdot \hat{\theta}_{viscoelastic}(i)) + B_{1b}$
    ▷ Viscosity of the damper $B_1$
  $\varepsilon$ = argmin (equation 9)
    ▷ Implicit Euler method
  $\hat{\theta}_{viscoelastic}(i) = (\varepsilon - \varepsilon_1) \cdot A_0$
    ▷ equation (10)
**end for**

t: time vector.

wide range of nonlinear dynamic systems, including time series. This makes NARX models a powerful tool in many different areas, including signal processing, control systems, and more. In particular, they have been used to model and analyze complex systems with nonlinear dynamics, such as financial markets, weather patterns, and biological systems. The flexibility and versatility of NARX models make them a valuable tool for a wide range of applications in science, engineering, and beyond [22].

To improve the performance of the NARX model in nonlinear time series prediction, it is important to take advantage of its memory capacity by incorporating past values of the predicted or true time series. The architecture of the NARX model is depicted in Fig. 12, which employs Tapped-Delay-Lines (TDLs) to create the network's dynamics.

There are two types of NARX neural network architectures, namely :

- Series-parallel architecture (open-loop), given by equation (12);
- Parallel architecture (close-loop), given by equation (13).

$$\hat{y}(t) = f\left[y(t), y(t-1), y(t-2), \ldots, y(t-n_y), u(t+1), u(t), u(t-1), \ldots, u(t-n_x)\right] \quad (12)$$

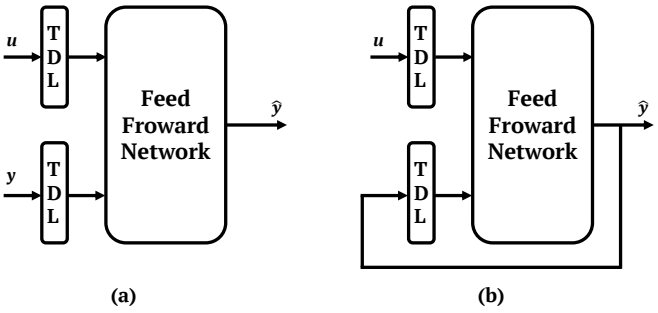


Fig. 12: Both NARX network architectures: **(a)** Series-parallel architecture; **(b)** Parallel architecture.

$$\hat{y}(t) = f\left[\hat{y}(t), \hat{y}(t-1), \hat{y}(t-2), \ldots, \hat{y}(t-n_y), u(t+1), u(t), u(t-1), \ldots, u(t-n_x)\right] \quad (13)$$

To implement the proposed model, two types of inputs are required: the target output of the neural network denoted $\theta$ and a set of inputs $R_{bending}$ that are specific to the system being modeled. The structure of the model, as defined in our study, is illustrated in Fig. 13.

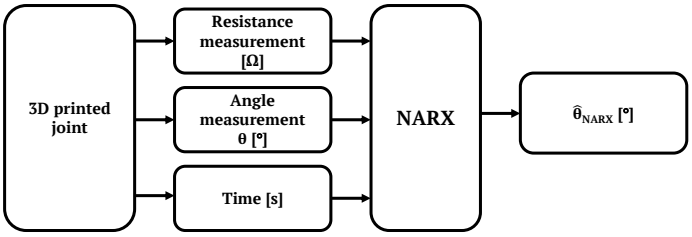


Fig. 13: Inputs and output for the proposed NARX neural network model, which the bending angle estimated by this model is denoted as $\hat{\theta}_{NARX}$.

The proposed model is implemented using the MATLAB 2021a software, utilizing a NARX model. The implementation follows Algorithm 2, as outlined below.

The parameters employed in programming this model are outlined in Table I. The necessary data was obtained by conducting measurements on the test bench depicted in Fig. 7.

**Algorithm 2** NARX model

1: Load data
▷ Resistance and angle measurement
2: Normalize data
3: Prepare data
▷ Convert the normalized data into ”tonndata” format
4: Choose training function
5: Create NARX network
▷ Use the ”narxnet” function
6: Prepare data for training and simulation
▷ Use the ”preparets” function
7: Set up data division
▷ Outlined in Table I
8: Train the network
▷ Use the ”train” function to train the network
9: Evaluate the performance of the trained model and analyze its predictions ▷ Using equations 5 and 6.

TABLE I: Parameters used in MATLAB Programming for proposed model.

| Parameters | Values |
|---|---|
| Training Function | Bayesian Regularization |
| Network performance | RMSE |
| Number of input delays | 2 |
| Number of feedback delays | 6 |
| Size of the hidden layers | 15 |
| Data used for training (%) | 70 |
| Data used for validation (%) | 15 |
| Data used for testing (%) | 15 |

With these settings, the input and target vectors are randomly partitioned into three distinct sets as described below:

- 70% of the data is allocated for training purposes.
- 15% of the data is reserved for validating the network's generalization and for halting the training process before overfitting.
- The remaining 15% of the data is utilized to independently test the network's generalization ability.

## V. Results and Discussion

### A. Experimental results related to textile conductive characterization

Initially, the resistance of the conductive textile alone is determined by assessing its behavior when subjected to stretching along its length using a test bench. This characterization process involves evaluating the conductive textile's resistance in both the weft and warp directions. In Fig. 14, the static characterization results of the conductive textile are presented, where the blue curve depicts a reduction in resistance as the conductive textile is stretched in the weft direction. It is worth noting that the length of stretching is fixed at 10 cm for both the warp and weft directions.

Nevertheless, when the conductive textile is stretched in the warp direction (as shown by the red curve in Fig. 14), it exhibits a parabolic response. This behavior renders the warp direction unsuitable for use as a sensor within the intended range. Consequently, a dynamic characterization is exclusively

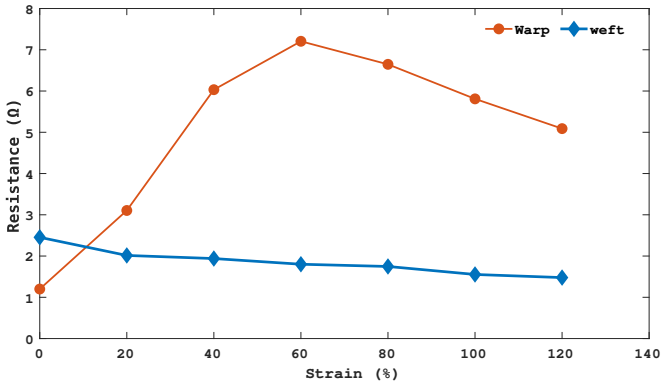


Fig. 14: Static characterization of the conductive textile, Resistance vs. strain in the weft and the warp direction.

conducted in the weft direction, which is considered more reliable for the desired purpose.

In the subsequent phase, the conductive textile attached to the elbow is characterized specifically in the weft direction. The objective is to detect movement by monitoring the change in resistance during stretching, as depicted in Fig. 15. This characterization process allows us to establish a relationship between resistance variations and movement, enabling the textile to serve as a reliable sensor.

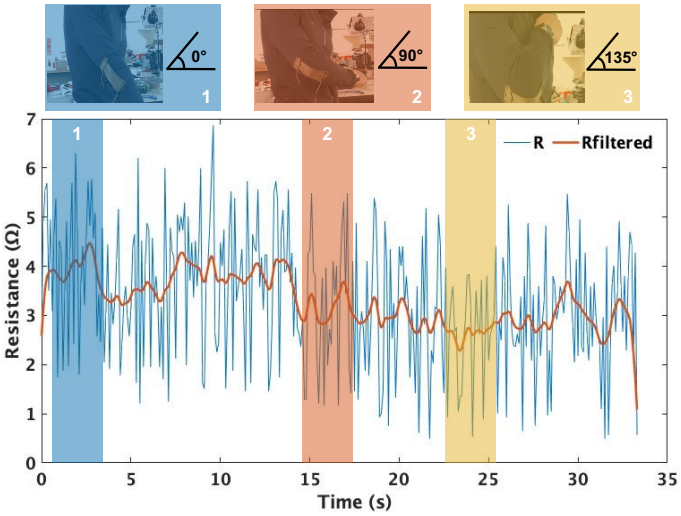


Fig. 15: Dynamic characterization of the conductive textile weft resistance as a function of time: **(1)** rest position; **(2)** mechanical bending (90°); **(3)** maximum bending (135°), where $R_{filtered}$ is filtered with a low-pass filter of order 2 and a cut-off frequency of 0.3Hz.

Fig. 15 provides a visualization of the dynamic characterization of a conductive textile. The plot illustrates the weft resistance of the textile (shown by the blue curve) and the corresponding filtered resistance (represented by the red curve).Although the signal remains free from noise, the desired signal exhibits an exceptionally low amplitude, presenting a significant challenge in detection.

During movements, peaks appear before the resistance decreases, making it challenging to identify the specific movement

and its progression. The resistances recorded are consistently close to 5 Ω, further complicating the interpretation of performed movements. Additionally, the sensor's behavior remains somewhat unstable, adding to the difficulty in accurately interpreting the detected movements.

However, while textiles alone may not possess sufficient piezoresistive properties to serve as standalone sensors, it has been observed that the resistance of the conductive textile remains relatively stable, typically around 4 Ω. This stability makes it an ideal candidate for use as a flexible and adaptable electrode within a garment-embedded sensor. Further details on this concept will be discussed in the subsequent section of this study.

### B. Experimental results related to the piezoresistive sensors

This section provides an overview of the experimental results obtained from the developed piezoresistive sensor, which was described in detail in Section III-A. The performance of the sensor was thoroughly evaluated through comprehensive characterization under both quasi-static and dynamic conditions.

*1) Quasi-static characterization:* Using the joint test bench shown in Fig. 7, the piezoresistive sensor was characterized to determine its resistance as a function of the bending angle. Quasi-static characterization was performed to avoid any viscoelastic effects, with a 3-minute waiting period between each data point. Consequently, eight different measurement tests were conducted on the studied sensor, and the dispersion and mean values were calculated.

For each data point, eight measurements were realized. From these measurements, the average resistance was calculated, represented by the dashed blue line on the blue graph in Fig. 16. The maximum error bar was calculated by subtracting the maximum measurement from the average, while the minimum error bar was calculated by subtracting the minimum measurement from the average.

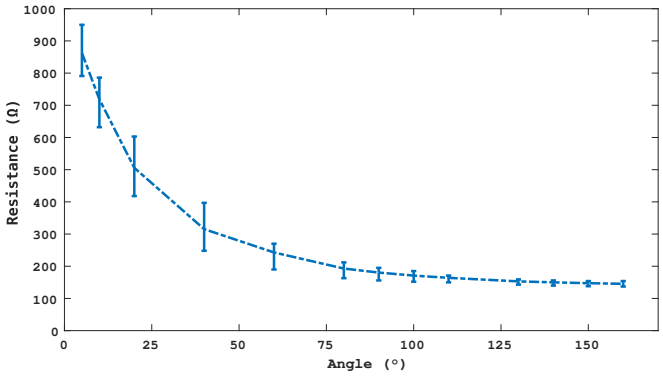


Fig. 16: Resistance vs. Mechanical Bending Angle ($\theta$) for the Piezoresistive Sensor (with error bars representing minimum and maximum values)

.

The results obtained in Fig. 16 illustrate the qualitative behavior of the sensor, which perfectly detect the resistance variations as a function of the angle. Furthermore, we conclude that the repeatability is the main unsolved problem of the Velostat. This is due to the differences observed in the 8 tests.

Subsequently, the sensor underwent continuous cycles of increasing and decreasing angles ranging from 0° to 160°, with a resting period of 3 minutes between each consecutive angle before measuring the resistance.

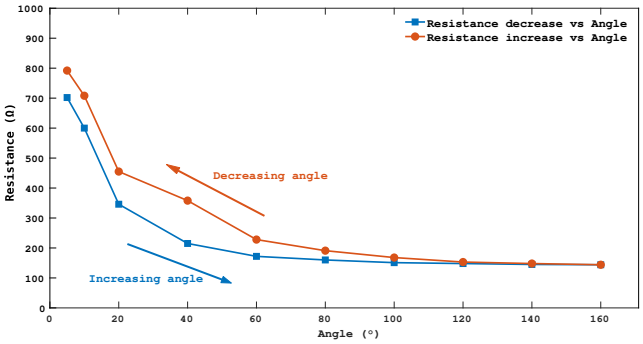


Fig. 17: The response of sensor to decreasing and increasing angle, as well as hysteresis trends.

The response of the sensor to increasing (blue curve) and decreasing (red curve) bending angles is illustrated in Fig. 17. As observed in previous characterizations [23], the sensor exhibits hysteresis in both responses, which can be largely attributed to viscoelasticity.

In this context, hysteresis refers to the maximum difference in output observed during the increasing and decreasing phases. To quantify this, the error was calculated as a percentage of the full-scale output using equation 14.

$$Hysteresis(\%) = \left| \frac{R_{increasing} - R_{decreasing}}{R_{max} - R_{min}} \right| \cdot 100\% \quad (14)$$

Here, $R_{\text{increasing}}$ and $R_{\text{decreasing}}$ represent the responses during ascending and descending bending, respectively, while $R_{\text{max}}$ and $R_{\text{min}}$ denote the maximum and minimum values of the sensor responses. The determination of hysteresis followed the same quasi-static characterization process.

*2) Dynamic characterization:* Fig. 18 depicts the dynamic characterization of the piezoresistive sensor's resistance, along with the corresponding angle $\theta$, as measured on the test bench. The red curve represents the applied rotation angle over time. Initially, the angle is set to zero, followed by progressively increasing dynamic variations. The blue curve illustrates the measured resistance response at the corresponding time instances. Notably, the resistance of the piezoresistive sensor decreases as a result of mechanical bending.

### C. Data processing and joint angle estimation

This section presents the results for both viscoelastic and NARX neural network models.

*1) Viscoelastic model:* The inverse viscoelastic model algorithm, as detailed in Section IV-A, is implemented for analysis. To initiate the parametric optimization process, an initial dataset, as shown in Fig. 19, is utilized. Subsequently, additional datasets will be introduced to evaluate the performance of the model.

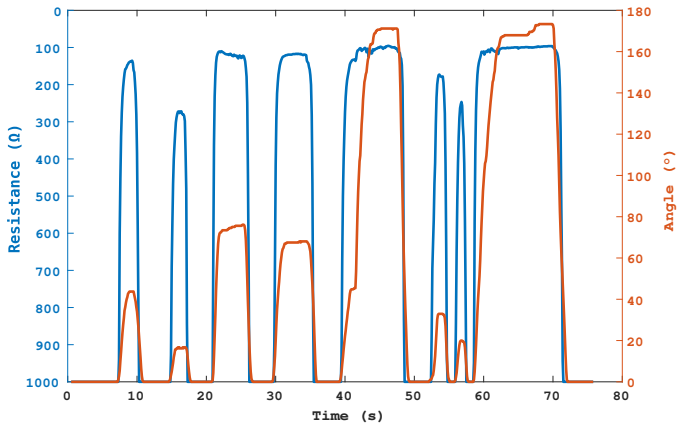


Fig. 18: The mechanical bending $\theta$ measured by the test bench and the dynamic resistance R vs. time.

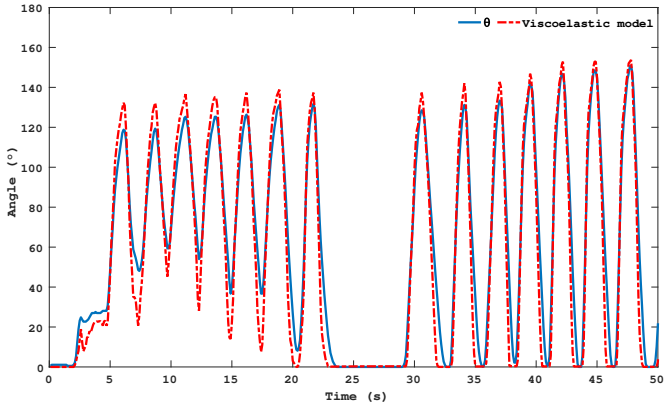


Fig. 19: Experimental angle $\theta$ and estimated angle of the viscoelastic model $\hat{\theta}_{viscoelastic}$ versus time.

The viscoelastic model provides a mechanical angle estimate with an RMSE of 12.88°, as demonstrated in Fig. 19. Although this error was calculated using the optimized dataset with a sample size of 6057, only 500 samples are displayed in the Fig. for brevity.

*2) NARX model:* The other model that has been implemented is the parallel architecture of the NARX model, as shown in the Fig. 20, with the parameters defined in Table I.

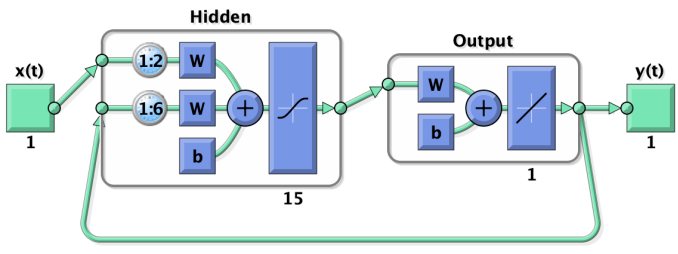


Fig. 20: Parallel architecture NARX model, where x is the electrical resistance and y is the estimated mechanical angle.

As it can be seen in Fig. 21, the NARX model can estimate correctly the mechanical angle with a RMSE = 4.85° calculated from validation data, and the angles tested are quite homogeneous, this graph also shows that the estimated angle has been underestimated for the lowest values.

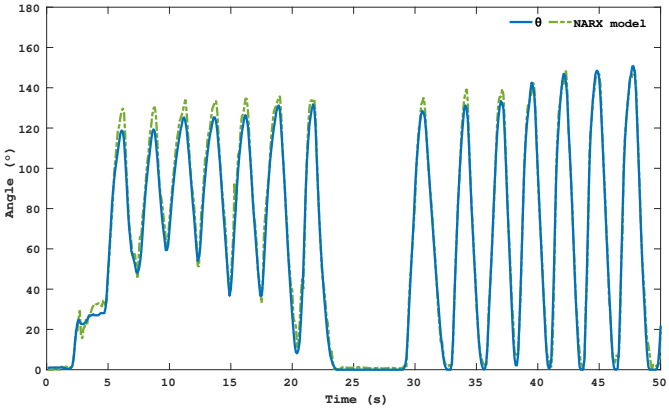


Fig. 21: Experimental angle $\theta$ and estimated angle of the NARX model versus time.

Comparing Fig. 19 and Fig. 21, it appears that the NARX model is more accurate for low angles, and has fewer overshoots for high values.

Fig. 22 shows that the majority of the errors are less than 5% for the NARX model, and it clearly indicates that the proposed NARX model is more accurate than the viscoelastic model.

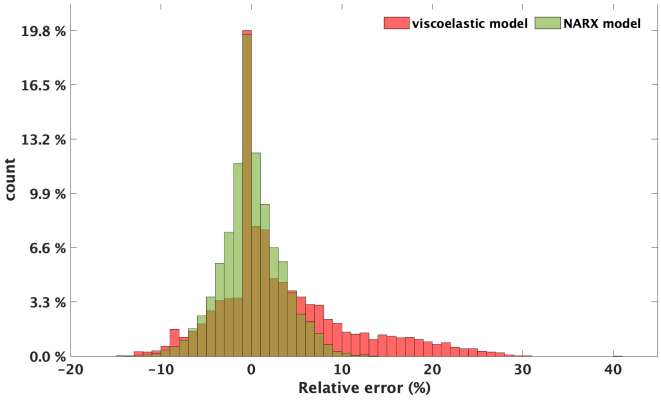


Fig. 22: Histogram of normalized data errors of both viscoelastic and NARX models.

The results obtained from the study indicate that the NARX neural network model shows a high degree of accuracy in estimating piezoresistive sensor data, achieving an impressive accuracy of approximately 5°. On the other hand, the viscoelastic model demonstrates an accuracy of nearly 13°. Such levels of accuracy position the proposed wearable garment as a credible alternative in the estimation of elbow and shoulder flexion angles, when compared to other solutions such as the OpenPose system with an RMSE of over 8° for right elbow flexion, or the Kinect system which records an RMSE exceeding 10° for the same task, as reported by [4].

## VI. Conclusions

In conclusion, this work presents a groundbreaking and cost-effective sensing system that utilizes flexible piezoresistive

sensors to accurately estimate the angle of upper body joints. We conducted a comprehensive comparative analysis of two models, a neural network, and a viscoelastic model, to process the sensor data, resulting in precise and reliable angle measurements.

The development of our garment, which incorporates piezoresistive sensors connected to an electronic board, offers a practical and portable solution for detecting resistance changes corresponding to joint movements. Notably, our study highlights the system's low energy consumption, ensuring extended use without frequent recharging.

The meticulous design and characterization of the piezoresistive sensors, utilizing a piezoresistive elastomer and a conductive textile, produced promising results with consistently reliable resistance measurements during both static and dynamic movements. This approach paves the way for numerous applications in healthcare, rehabilitation, and various other fields where accurate joint angle measurement is essential.

Overall, the perspectives for this research are exciting and wide-ranging, with potential applications in various fields. The low power consumption of the proposed system makes it a potential candidate to be power from harvested energy, thus shifting forward the paradigm of wearable sensors towards more integrated and comfortable solutions.

## Aknowledgment

The authors express their sincere gratitude to Ms. Rozenn Jodin for her invaluable technical assistance in prototyping the integrated textile sensors.

## References

[1] G. Aroganam, N. Manivannan, and D. Harrison, "Review on wearable technology sensors used in consumer sport applications," Sensors, vol. 19, no. 9, 2019. [Online]. Available: https://www.mdpi.com/1424-8220/19/9/1983

[2] S. Beg, M. Handa, R. Shukla, M. Rahman, W. H. Almalki, O. Afzal, and A. S. A. Altamimi, "Wearable smart devices in cancer diagnosis and remote clinical trial monitoring: Transforming the healthcare applications," Drug Discovery Today, vol. 27, no. 10, p. 103314, 2022. [Online]. Available: https://www.sciencedirect.com/science/article/pii/S1359644622002835

[3] M. H. Iqbal, A. Aydin, O. Brunckhorst, P. Dasgupta, and K. Ahmed, "A review of wearable technology in medicine," Journal of the Royal Society of Medicine, vol. 109, no. 10, pp. 372–380, 2016, pMID: 27729595. [Online]. Available: https://doi.org/10.1177/0141076816663560

[4] W. Kim, J. Sung, D. Saakes, C. Huang, and S. Xiong, "Ergonomic postural assessment using a new open-source human pose estimation technology (openpose)," International Journal of Industrial Ergonomics, vol. 84, p. 103164, 2021. [Online]. Available: https://www.sciencedirect.com/science/article/pii/S0169814121000822

[5] Catapult, "Catapult sports. (n.d.). about us. retrieved april 11, 2023, from," https://www.catapultsports.com/about-us/.

[6] Vicon, "Vicon motion systems ltd. (n.d.). about us. retrieved april 11, 2023, from," https://www.vicon.com/about-us.

[7] Qualisys, "Qualisys ab. (n.d.). about us. retrieved april 11, 2023, from," https://www.qualisys.com/about-us/.

[8] D. Hoareau, X. Fan, F. Abtahi, and L. Yang, "Evaluation of in-cloth versus on-skin sensors for measuring trunk and upper arm postures and movements," Sensors, vol. 23, no. 8, 2023. [Online]. Available: https://www.mdpi.com/1424-8220/23/8/3969

[9] Z. Zhang, X. Gui, Q. Hu, L. Yang, R. Yang, B. Huang, B.-R. Yang, and Z. Tang, "Highly sensitive capacitive pressure sensor based on a micropyramid array for health and motion monitoring," Advanced Electronic Materials, vol. 7, no. 7, p. 2100174, 2021. [Online]. Available: https://onlinelibrary.wiley.com/doi/abs/10.1002/aelm.202100174

[10] X. Yue, R. Lu, Q. Yang, E. Song, H. Jiang, Y. Ran, and B.-O. Guan, "Flexible wearable optical sensor based on optical microfiber bragg grating," Journal of Lightwave Technology, vol. 41, no. 6, pp. 1858–1864, 2023.

[11] X. Guan, B. Xu, and J. Gong, "Hierarchically architected polydopamine modified batio3@p(vdf-trfe) nanocomposite fiber mats for flexible piezoelectric nanogenerators and self-powered sensors," Nano Energy, vol. 70, p. 104516, 2020. [Online]. Available: https://www.sciencedirect.com/science/article/pii/S2211285520300732

[12] E. Jeong, J. Lee, and D. Kim, "Finger-gesture recognition glove using velostat (ICCAS 2011)," p. 5.

[13] Q. Yu, P. Zhang, and Y. Chen, "Human motion state recognition based on flexible, wearable capacitive pressure sensors," Micromachines, vol. 12, no. 10, 2021. [Online]. Available: https://www.mdpi.com/2072-666X/12/10/1219

[14] D. Wang, B. Sheng, L. Peng, Y. Huang, and Z. Ni, "Flexible and optical fiber sensors composited by graphene and pdms for motion detection," Polymers, vol. 11, no. 9, 2019. [Online]. Available: https://www.mdpi.com/2073-4360/11/9/1433

[15] F. Mokhtari, G. M. Spinks, C. Fay, Z. Cheng, R. Raad, J. Xi, and J. Foroughi, "Wearable electronic textiles from nanostructured piezoelectric fibers," Advanced Materials Technologies, vol. 5, no. 4, p. 1900900, 2020. [Online]. Available: https://onlinelibrary.wiley.com/doi/abs/10.1002/admt.201900900

[16] Y. Zhang, Y. Huang, X. Sun, Y. Zhao, X. Guo, P. Liu, C. Liu, and Y. Zhang, "Static and dynamic human arm/hand gesture capturing and recognition via multiinformation fusion of flexible strain sensors," IEEE Sensors Journal, vol. 20, no. 12, pp. 6450–6459, 2020.

[17] Z. A. Abro, Z. Yi-Fan, C. Nan-Liang, H. Cheng-Yu, R. A. Lakho, and H. Halepoto, "A novel flex sensor-based flexible smart garment for monitoring body postures," Journal of Industrial Textiles, vol. 49, no. 2, pp. 262–274, 2019. [Online]. Available: https://doi.org/10.1177/1528083719832854

[18] Velostat, "Film, velostat, 36 x 150 roll 67y8891." https://datasheet.octopart.com/170436X150-SCS-datasheet15984175.pdf/, accessed: 20.04.2022.

[19] A. Dzedzickis, E. Sutinys, V. Bucinskas, U. Samukaite-Bubniene, B. Jakstys, A. Ramanavicius, and I. Morkvenaite-Vilkonciene, "Polyethylene-carbon composite (velostat®) based tactile sensor," Polymers, vol. 12, no. 12, 2020. [Online]. Available: https://www.mdpi.com/2073-4360/12/12/2905

[20] STATEX-Shieldex-Techniktex, "Statex shieldex techniktex p130 + b()," https://www.shieldex.de/products/shieldex-technik-tex-p130-b/, (accessed: 20.04.2022).

[21] A.-R. A. Laaraibi, G. Jodin, D. Hoareau, N. Bideau, and F. Razan, "Flexible dynamic pressure sensor for insole based on inverse viscoelastic model," IEEE Sensors Journal, vol. 23, no. 7, pp. 7634–7643, 2023.

[22] Z. Boussaada, O. Curea, A. Remaci, H. Camblong, and N. Mrabet Bellaaj, "A nonlinear autoregressive exogenous (narx) neural network model for the prediction of the daily direct solar radiation," Energies, vol. 11, no. 3, 2018. [Online]. Available: https://www.mdpi.com/1996-1073/11/3/620

[23] M. Hopkins, R. Vaidyanathan, and A. H. Mcgregor, "Examination of the performance characteristics of velostat as an in-socket pressure sensor," IEEE Sensors Journal, vol. 20, no. 13, pp. 6992–7000, 2020.

**Abdo-rahmane Anas LAARAIBI** was born in Casablanca, Morocco in 1996. He received his first M.S degree in Automation-Signal Processing-Computer Science from Hassan 1er University, Settat, MA in 2020 and his second M.S degree in Signal Image from Rennes 1 University, Rennes, FR in 2021. He is currently a PhD student in Mechatronic Engineering at Ecole Normale Supérieure de Rennes, IETR group and SATIE laboratory of Rennes.

His research focuses on the development of an autonomous integrated instrumentation allowing the quantification of an athlete's movements for indoor sports

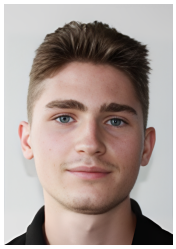

**Corentin Depontailler** born in Troyes, France, earned Bachelor's degrees in Electronics, Electrical Energy and Automation (EEEA) and Science for Engineering (SPI) from the Mechatronics Department of the Ecole Normale Supérieure of Rennes in 2022. He is currently pursuing a Master's degree in Sciences for the Engineer and Applications (SPIA) at the same institution and has conducted extensive research on the development and evaluation of textile piezoresistive sensors. This research involved fabricating and characterizing the sensors, designing a smart wearable garment that incorporates these sensors, and integrating them into the garment. Additionally, Corentin has investigated the energy consumption of the system and explored the sensors' ability to detect human motion. Through this work, he has gained a deep understanding of the capabilities and limitations of textile-based piezoresistive sensors and their potential applications in wearable technology.

**Gurvan JODIN** received the B.S. in both mechanical engineering and electrical engineering, from Rennes 1 University, France, in 2011. He received the M.Ed in mechatronics from Ecole Normale Supérieure de Rennes, and was major of the 2013 "agrégation" teacher competitive recruitment of Industrial Science for Engineering. He received the Ph.D. degree from Polytechnic National Institute of Toulouse, France, in electrical engineering and aerodynamics. After postdocs at Mechanical Engineering Department at Massachusetts Institute of Technology, Boston, MA, USA, and at Ecole Normale Supérieure de Rennes, he is currently associate professor with SATIE laboratory at Ecole Normale Supérieure de Rennes, France. His research interests are in eco-co-design complex mechantronics systems. This includes topics in experimental approach, mechatronics, hydrodynamics, sensors, power electronics and smart grids.

**Damien HOAREAU** received the B.S. degree in both mechanical engineering and electrical engineering, from Rennes 1 University, France, in 2017. He received the M.S and M.Ed degree in mechatronics from Ecole Normale Supérieure de Rennes in 2018 and 2019. He received the Ph.D. degree from Ecole Normale Supérieure de Rennes, France, in electrical engineering in 2023. His research interest includes the development of sensing system for sport science and signal processing to monitor athlete parameters to improve performance.

**Nicolas BIDEAU** was born in France in 1978. He received the bachelor degree in Mathematics from the University of Brest, France, the applied mathematics degree and the mechanics degree from the university Rennes 1. He received the PhD degree in Mechanics from the University Rennes 1, France, in 2009. In 2009 he joined the University of Technology of Compiègne, France as a postdoctoral researcher in biomedical engineering. Since 2011, he is an assistant professor in biomechanics at the department of sports sciences from the University Rennes 2. His current research interests, as member of the Movement, Sports and Health (M2S) laboratory, include movement analysis, modeling end experimental biomechanics with applications to sports sciences. His main applications focus on biomechanical analysis of the musculoskeletal system from optoelectronic or IMU based motion capture as well as the analysis of the athlete's material and environmental interactions.

**Florence RAZAN** received a master in physic and electronic in 2002 and a PhD in microsystems of Bordeaux University (France) in 2005. From 2006 to 2020, she was an associate professor with the mechatronic department at ENS Rennes and in SATIE laboratory. She is currently professor at ENS Rennes and IETR group. Her teams interest concerns the development of autonomous biosourced microsystems for movement characterization. Her current work focuses on the development of autonomous and biosourced embedded communicating systems as an interface between humans or humanoid robots and their environment. The main challenges concern the system architecture, the design of autonomous sensors, the integration of an energy recuperator and the development of low-power electronics. Her main research interests focuse on the development of piezoelectric transducers.